ACS APPLIED MATERIALS & INTERFACES

www.acsami.org

Forum Article

Femtomolar Detection of Thrombin in Serum and Cerebrospinal Fluid via Direct Electrocatalysis of Oxygen Reduction by the Covalent G4-Hemin-Aptamer Complex

Kamila Malecka and Elena E. Ferapontova*

Cite This: https://doi.org/10.1021/acsami.1c03784

Read Online

ACCESS | Metrics & More | Article Recommendations | Supporting Information

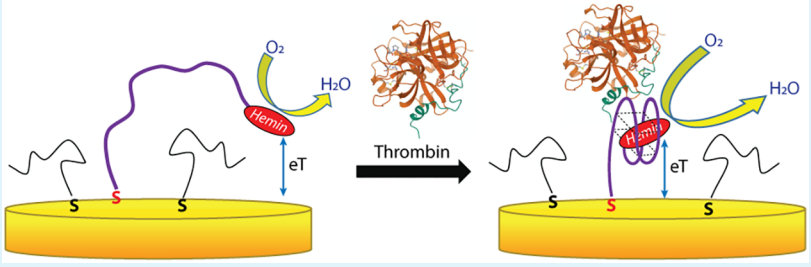

ABSTRACT: Thrombin, a serine protease playing a central role in the coagulation cascade reactions and a potent neurotoxin produced by injured brain endothelial cells, is a recognized cardiac biomarker and a critical biomarker for Alzheimer's disease development. Both in vivo and in vitro, its low physiological concentrations and nonspecific binding of other components of physiological fluids complicate electroanalysis of thrombin. Here, femtomolar levels of thrombin in serum and an artificial cerebrospinal fluid (CSF) were detected by the indicator-free electrochemical methodology exploiting the O_2 reduction reaction directly, with no electron transfer mediators, electrocatalyzed by the covalent G4-hemin DNAzyme complex naturally self-assembling upon thrombin binding to the hemin-modified 29-mer DNA aptamer sequence tethered to gold via an alkanethiol linker. Coadsorbed PEG inhibited nonspecific protein binding and allowed the sought signal resolution. The proposed assay exploiting the "oxidase" activity of G4-hemin DNAzyme does not require any coreactants necessary for the traditional peroxidase activity-based assays with this DNAzyme, such as H_2O_2 and redox mediators, or solution deaeration and allows fast, overall 30 min analysis of thrombin in aerated buffer, CSF, and 1% human serum solutions. This pioneer approach exploiting the oxidase activity G4-hemin DNAzyme is simple, sensitive, and selective and represents a new tool for ultrasensitive electrocatalytic assays based on simple and efficient O_2-dependent DNAzyme labels.

KEYWORDS: *electrocatalysis, thrombin, aptamer, DNAzyme, G4-hemin covalent complex, biosensor*

INTRODUCTION

More than 36 million people worldwide live with Alzheimer's disease (AD), an age-related neurodegenerative dementia, and this number is expected to reach 66 million in 2030, which puts enormous burden on society and health-care institutions.[1] Postulated neurovascular damage of the brain is considered a characteristic feature of the disease, which contributes to its pathogenesis and progression and shares the same risk factors as vascular diseases.[2,3] Hypoxia, oxidative stress, and metabolic changes induced by cardiovascular risk factors activate the endothelial cells of the brain microvasculature then generating inflammatory cytokines, growth factors, and neurotoxic proteins.[4] Unsurprisingly, efforts are focused on finding disease-modifying anti-inflammatory therapies not yet available.

Recently, thrombin, a serine protease playing a central role in coagulation cascade reactions, hemostasis, and thrombosis and an important cardiac biomarker,[5] was also suggested as a possible target for AD therapy, in which inhibitors suppress thrombin-mediated diabetes- and hypoxia-induced cerebrovascular effects and improve cognition in AD patients.[6] In suggested treatments, thrombin is considered as a critical biomarker of the disease development: it is a potent neurotoxin produced by injured brain endothelial cells, and in AD, thrombin levels are elevated both in the brain and cerebral microvasculature, which causes pro-inflammatory effects.[6]

Hitherto, numerous electrochemical and optical aptamer-based biosensors[7] for the detection of thrombin as a biomarker of thromboembolic and hemorrhagic diseases and even cancer

Special Issue: Materials Applications of Aptamers

Received: February 26, 2021
Accepted: April 7, 2021

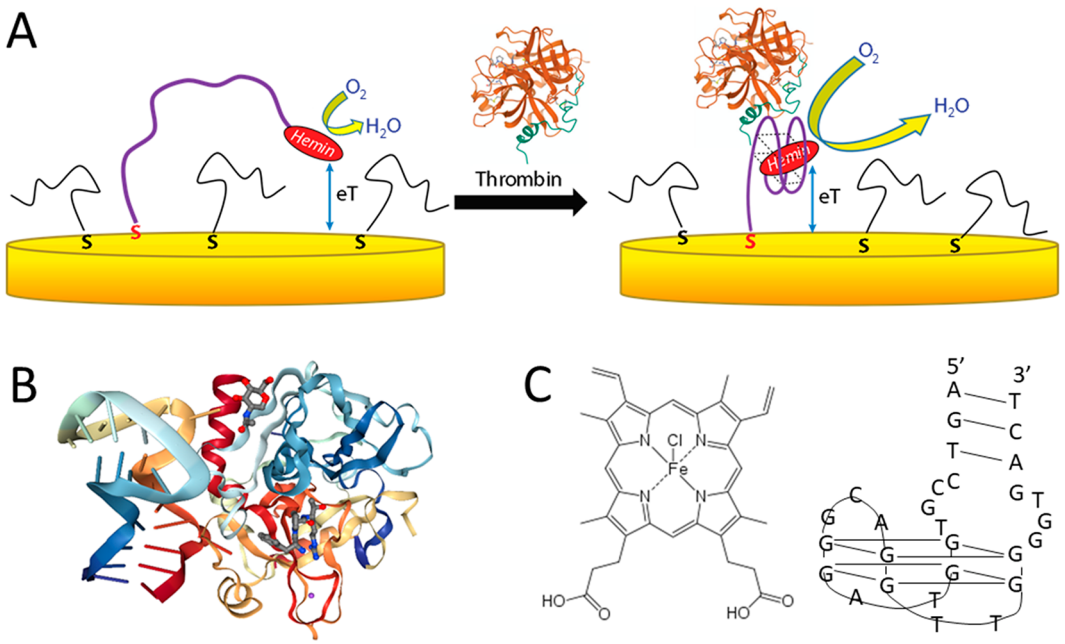

Figure 1. (A) Schematic representation of the O_2-dependent electrocatalytic detection of α-thrombin: the hemin-modified thiolated aptamer is immobilized on the gold electrode altogether with thiolated PEG and directly (with no mediators) electrocatalyzes the O_2 reduction; binding of thrombin (image from the RCSB PDB (rcsb.org) of PDB ID: 1PPB)[22] triggers G4-hemin self-assembly with enhanced electrocatalytic properties for O_2 reduction, which is electrochemically detected. (B) Crystal structure of the complex formed between the aptamer sequence and human α-thrombin, image from the RCSB PDB (rcsb.org) of PDB ID: 4I7Y,[21] and (C) the hemin structure and the aptamer sequence fold in the thrombin-bound state: hemin binds between two G4 planes.

development[5,8−10] has been reported. Most of them aim at sensitivities sufficient for robust analysis in blood/serum, where blood coagulation-related concentrations of free thrombin vary between less than 1 nM and more than 500 nM.[11] Already the pioneering reports on the indicator-free electrochemical detection of thrombin by redox-labeled aptamer beacons addressed this challenge of the nanomolar analysis of thrombin in serum.[12,13] Neurological applications require different assay sensitivities and limits of detection (LOD). In the brain, 10 nM to 10 μM thrombin induces neuronal cell death, whereas at 10 pM to 10 nM levels, thrombin protects cells from oxygen and glucose deprivation, reactive oxygen species, and hypoglycemia.[14,15]

Currently, just a few electrochemical aptamer-based sensors show sufficiently low LOD in serum.[16−19] However, they use quite complex interfacial and reactant/catalytic labels designs such as Co-MOF decorated with PtPd nanoparticles (NPs),[18] peptide-Pt NP@reduced graphene oxide bioconjugates,[19] Pt and MnO_2 NP-modified MWCNT labels,[16] and other similarly complex modifications and, eventually, assay protocols,[7,20] which make them less suitable for immediate clinical applications.

In this work, we suggest a new electrocatalytic methodology for the fast and inexpensive ultrasensitive detection of thrombin that exploits the natural pseudo-G-quadruplex (G4) self-assembly of the thrombin-specific aptamer sequence triggered by the thrombin-aptamer binding[21] and its oxidase activity (i.e., its reactivity with O_2 as electron acceptor) for the electrocatalytic signal amplification (Figure 1).

In the presence of hemin, the aptamer-thrombin binding results in the formation of the G4-hemin complex, also known as a "peroxidase-mimicking" DNAzyme exhibiting a peroxidase activity in the presence of H_2O_2 and such typical peroxidase substrates as catechols or ABTS.[23] The peroxidase activity of this DNAzyme has been successfully used for optical (nanomolar range)[24] and electrochemical (picomolar range)[25,26] detections of thrombin. Therewith, the H_2O_2-dependent DNAzyme assays always require a three-component reagent system present in solution: hemin (usually, at its 1 μM levels), H_2O_2, and relevant optically or electrochemically active peroxidase substrates, plus deaeration of the working solutions, since O_2 reduction interferes with H_2O_2-based electroanalysis.[27] In addition, such low hemin concentrations, close to hemin-G4's K_d, destabilize the DNAzyme complex and result in its partial dissociation,[28] responsible both for the unsatisfactory sensitivity of DNAzyme assays and artifacts associated with the electrocatalytic activity of free hemin in reaction with H_2O_2.[29]

Recently, we have demonstrated a remarkable property of covalent G4-hemin complexes to directly (i.e., in the absence of any redox mediators, in the direct electron transfer (ET) reaction between the electrode and the heme) electrocatalyze the reaction of O_2 reduction, introducing it as a more advantageous indicator reaction because it does not need any extra (co)substrate or solution deaeration.[29] The covalent G4-hemin complexes showed improved DNAzyme stability and integrity[28] and allowed not only indicator-free peroxidase DNAzyme activity (no hemin or substrates and mediators present in solution) but also O_2-dependent oxidase activity of DNAzyme at potentials exceeding those of free hemin.[29] A similar O_2-dependent bioelectrocatalysis of heme proteins, such as bacterial and plant hemoglobins, was shown to be superior to the peroxidase one, with its onset approaching the potentials of H_2O_2 bioelectrocatalysis.[30,31] Thus, by analogy to heme proteins, it was suggested that the O_2-dependent electrocatalytic activity of the covalent G4-hemin complexes might allow simpler and faster electrocatalytically amplified

https://doi.org/10.1021/acsami.1c03784
ACS Appl. Mater. Interfaces XXXX, XXX, XXX−XXX

analysis of thrombin both in serum and in a cerebrospinal fluid (CSF) (Figure 1).

Here, we explored the ability of the covalent hemin-G4 complexes to directly, with no mediators, electrocatalyze the O_2 reduction reaction for electrochemical sensing of thrombin. In the aptasensor development, we used a 29-mer sequence HD22 5′-AGT CCG TGG-TAG GGC AGG TTG GGG TGA CT-3′ adopting a mixed duplex−quadruplex conformation upon thrombin binding (Figure 1B, C)[32] and bearing thiol and amine modifications for electrode immobilization and hemin bioconjugation. We show that only at the mixed aptamer/poly(ethylene glycol) (PEG) self-assembled monolayers (SAMs) does the DNAzyme electrocatalysis of O_2 reduction induced by thrombin binding to the hemin-modified aptamer allow down to 1 fM thrombin detection in serum and artificial CSF.

MATERIALS AND METHODS

Materials. Hemin, poly(ethylene glycol) methyl ether thiol (PEG-SH; $CH_3O(CH_2CH_2O)_nCH_2CH_2SH$, $M_n \sim 6000$), 1-mercaptohexanol, 33% H_2O_2, ethyl carbodiimide hydrochloride (EDC), sulfo-*N*-hydroxysuccinimide (NHS), bovine serum albumin (BSA) and human serum (sterile-filtered, from male AB plasma, Lot 121 K16972; stored at −20 °C), dimethyl sulfoxide (DMSO), guanidinium chloride, urea, and all buffer solution components, KH_2PO_4/K_2HPO_4, NaCl, and NaOH, were purchased from Sigma-Aldrich (Broendby, Denmark). Thiolated ethylene glycol SH-C_6-$(EG)_2$-OH was from ProChimia Surfaces (Poland) and ethanol was from VWR Chemicals (Poland). The thrombin-specific DNA aptamer sequence 5′-SH-C6-AGT CCG TGG TAG GGC AGG TTG GGG TGA CTT TTT TTT TTT-C7-NH_2-3′[32] (a spacer underlined) was synthesized by Metabion (Planegg, Germany, Figure S1). Native human α-thrombin (MW 36.7 kDa, pI 7, 7.3, and 7.6,[33] 10.1 mg mL^{-1} solution in 50% water:50% glycerol) was from Thermofisher Scientific (USA). Ultrapure water from a Millipore Milli-Q Reference A+ system (18 MΩ cm) was used for preparing all solutions. All experiments were performed at rt (21 °C ± 1).

Hemin Conjugation to the Aptamer. Hemin was conjugated to the aptamer sequence by the EDC/NHS coupling reaction between the amine group of DNA and hemin's propionic acid carboxylic group,[34] under the 37-fold hemin excessive conditions resulting in the monoadduct formation, with a slightly modified protocol.[35] For this, 18 μL of 150 μM DNA stock solution in 0.1 M phosphate buffer, pH 7.0, was mixed with 20 μL of 5.6 mg mL^{-1} NHS, 20 μL of 96 mg mL^{-1} EDC, and 18 μL of 5 mg mL^{-1} hemin solutions in DMSO, to provide their final concentrations of 100, 5, and 1 mM, respectively (27 μM DNA final concentration). The mixture was incubated for 2 h (this time provided the highest efficiency of the hemin-DNA bioconjugation reaction, Figure S2) and then dialyzed overnight using a 1 kDa cutoff membrane (GE Healthcare) to remove excessive hemin.

Electrode Modification with the Aptamer. Prior to modification, 2 mm diameter gold disk electrodes (CH Instruments, Austin, TX) were cleaned by potential cycling in 0.5 M NaOH (from −0.5 to −1.4 V, scan rate 0.05 V s^{-1}, 10 cycles) and successively mechanically polished on microcloth pads (Buehler, Germany) in 1 μm diamond and 0.1 μm alumina slurries (Struers, Denmark), for 2 min in each. After that, the electrodes were 10 min ultrasonicated in a 1:1 water−ethanol mixture, followed by electrochemical cleaning in 1 M H_2SO_4 (the potential range between −0.3 and +1.7 V, at 0.3 V s^{-1}, 10 cycles), and then in 0.5 M H_2SO_4 containing 10 mM KCl (from 0 to +1.7 V, also 10 cycles). The electrochemically active surface area of gold electrodes evaluated from surface-oxide reduction peaks in the last CV scan in 0.1 M H_2SO_4 (12 cycles in total) was 0.12 ± 0.01 cm^2. Then electrodes were rinsed with water, kept in absolute ethanol for 30 min, and dried in a N_2 flow prior to modification. For aptamer immobilization, 1 μL of a 27 μM stock solution of the hemin-conjugated aptamer was diluted in 20 mM phosphate buffer solution (PB) containing 150 mM NaCl, pH 7.4 (PBS), to a 0.1 μM final concentration, and 10 μL of this solution were placed on the electrode surface, covered with a lid, and left for 2 h. After immobilization, aptamer-modified electrodes were rinsed with PBS, dried in the nitrogen flow, kept for 10 min in 1 mM solution of PEG-SH (or any other 1 mM thiol used; in first trials, a 30 min modification) in PBS, carefully washed with PBS, and left for 30 min in PBS before electrochemical measurements. If not immediately used, the aptamer-modified electrodes were stored in PBS at 4 °C and used, with no apparent loss of their thrombin binding activity, within 1 week after their preparation.

Electrochemical Measurements. Cyclic voltammetry (CV) and chronocoulometry (CC) were performed in a standard three-electrode 25 mL electrochemical cell placed inside the Faraday cage and connected to the potentiostat (PGSTAT101, Eco Chemie, Utrecht, Netherlands) supported with NOVA 1.8 software. The DNA-modified gold was the working electrode, an Ag/AgCl (3 M KCl) was the reference electrode and a Pt wire was the auxiliary electrode. CC measurements were carried out with a pulse period of 1 s at −0.4 V. For thrombin analysis, aptamer-modified electrodes were 30 min incubated in 1 to 1000 fM α-thrombin solutions in 20 mM PBS, pH 7.4, and then immediately electrochemically interrogated in the same cell. This incubation time was earlier shown to be sufficient to ensure the analytically significant aptamer-protein binding both on surface[12,13,36,37] and in solution.[38] Shorter incubation times, more relevant for analysis in flow-injection systems,[39] were not investigated here. Alternatively, either 1% serum diluted with the same buffer or the artificial cerebrospinal fluid (CSF: 108 mM NaCl, 2.5 mM KCl, 8.2 mM $MgCl_2$, 2 mM $CaCl_2$, 4 mM $NaHCO_3$, 1 mM Na_2HPO_4, 10 mM glucose), pH 7.4,[40] were used as supporting electrolytes. As a negative control, 0.53, 5.30, and 15.15 μM BSA was used. If not specified otherwise, working solutions were 2 min air-equilibrated before each electrocatalytic CV recording to avoid depletion of O_2 near the electrode surface during consecutive measurements; such O_2 depletion was not observed with CC analysis. The surface coverage with the aptamer-hemin conjugate Γ, mol/cm^2, was calculated by integrating the hemin peak surface areas in CV, $Q = nFA\Gamma$, where Q is the reaction-associated charge, F and A represent Faraday's constant and the electrode surface area, and n is the number of electrons involved in the reaction. At least five identically modified electrodes were interrogated in each set of experiments. Recovery analysis was performed in triplicate for each spike concentration.

RESULTS AND DISCUSSION

Design of the Aptamer Sequence. Two modifications of the aptamer sequence, the thiol-C_6 modification at 5′ end and the dT_{10} spacer-C_7-amine modification introduced for hemin conjugation at its 3′ end, did not interfere with the thrombin-binding site (Figure 1C). The length of the dT_{10} spacer was shown to provide the flexibility of the covalently attached hemin sufficient for productive G4-hemin interactions.[41] Shorter spacers probed did not allow stable complex formation because of a spatial hindrance of intermolecular interactions.

Electrocatalysis of O_2 Reduction by the Hemin-Aptamer-Modified Gold Electrodes. To develop an aptasensor based on the O_2-dependent activity of the covalent G4-hemin complexes, we first interrogated electrocatalysis of O_2 reduction with the hemin-conjugated aptamer coadsorbed on gold electrodes with (i) mercaptohexanol, a traditional gold surface space-filler,[19,25,36] and (ii) thiolated PEGs known to prevent nonspecific adsorption of proteins:[37,42] thiolated di(ethylene glycol) SH-C_6-$(EG)_2$-OH (diEG-SH) and thiolated poly(ethylene glycol) $CH_3O(CH_2CH_2O)_nCH_2CH_2SH$, $M_n \sim 6000$ (PEG-SH).

All hemin-conjugated aptamer-modified electrodes produced a distinct wave of electrocatalytic reduction of O_2, starting from 30 mV on diEG-modified electrodes and −200 mV on

https://doi.org/10.1021/acsami.1c03784
ACS Appl. Mater. Interfaces XXXX, XXX, XXX−XXX

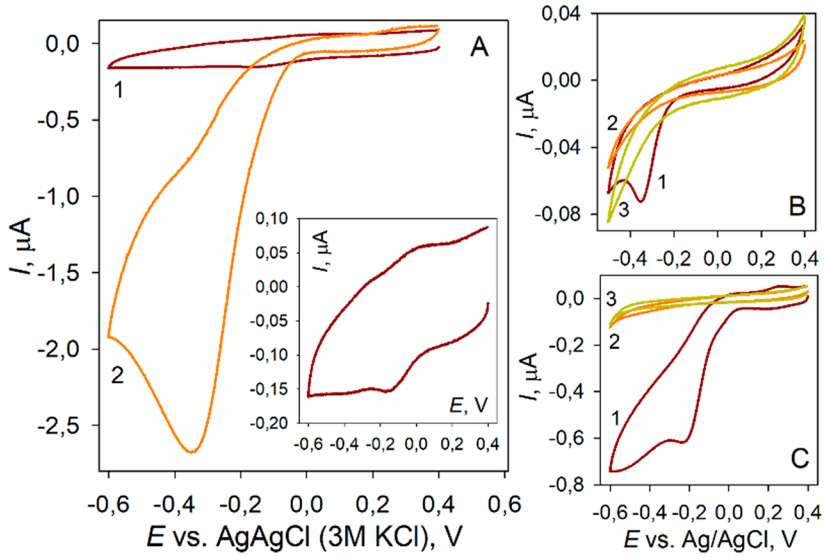

Figure 2. Representative CVs recorded in 20 mM PBS/0.15 M NaCl, pH 7.4, with the hemin-conjugated aptamer- and (A) PEG-, (B) mercaptohexanol-, and (C) diEG-modified gold electrodes. In (A): (1) deaerated and (2) aerated solutions (inset: enlarged (1)), and in (B, C): (1) aerated solutions before and after incubation with (2) 1 nM thrombin and (3) 15.15 μM BSA. Scan rate: 10 mV s^{-1}.

mercaptohexanol-modified electrodes (Figure 2B, C). The onset potential for electrocatalysis and its efficiency (the electrocatalytic currents) were consistent with permeability of the mixed SAMs for O_2 reduction. The electrocatalytic currents were ca. 10-fold lower on the mercaptohexanol SAMs, apparently providing better blocking of the electrode surface than diEG SAMs. In the absence of the coadsorbed aptamer, the mercaptohexanol SAM impeded the O_2 reduction reaction, particularly, compared to the bare gold electrodes (Figure S3). Thus, the observed electrocatalytic responses resulted solely from O_2 reduction electrocatalyzed by the DNA-conjugated hemin undergoing the direct ET transformation on the electrode.

In the absence of thrombin, the aptamer-conjugated hemin electrocatalyzed O_2 reduction in aerated solutions according to[43]

$$\text{Fe(III)Porph} + 1e^- \rightarrow \text{Fe(II)Porph} \quad \text{(a)}$$

$$4\text{Fe(II)Porph} + O_2 + 4H^+ \rightarrow 4\text{Fe(III)Porph} + 2H_2O \quad \text{(b)}$$

where reaction b proceeds via formation of H_2O_2 as intermediate. The electrocatalytic reactions a and b, observable even in the presence of trace amounts of hemin,[44] might complicate analysis of thrombin, unless the signals from the G4-hemin complex formed after thrombin binding exhibit either a different or enhanced electrocatalytic pattern in the reaction of O_2 reduction, as was previously shown for hemin-protein and hemin-DNA complexes whose higher oxidation states are stabilized by either protein[31,45] or G4 matrices.[29]

However, contrary to expectations, thrombin binding inhibited direct electrocatalysis of O_2 reduction by the formed G4-hemin DNAzyme both on the mercaptohexanol- and diEG-modified electrodes (Figure 2B, C, curve 2). On the other hand, very similar effects were produced by binding of BSA (Figure 2B, C, curve 3). Thus, we assigned the observed inhibition of electrocatalytic responses to the essential nonspecific binding of both proteins to the mercaptohexanol- and diEG-modified electrodes. Such surface blocking by proteins prohibited direct ET between the electrode and both the G4-hemin complex and the original thrombin-unbound aptamer-conjugated hemin, and, as a result, direct electrocatalysis of the O_2 reduction reaction.

The antifouling properties of the mixed aptamer-thiol SAMs were improved when PEG-SH with a larger PEG content was used. The PEG-modification eventually boosted electrocatalysis of O_2 reduction compared to the mercaptohexanol and diEG mixed SAMs (Figure 2A), very likely due to the enhanced H_2O absorption (a product of electrocatalysis) by hydrophilic PEG, consistent with previous reports.[46,47] The pronounced wave of the electrocatalytic reduction of O_2 by the aptamer-conjugated hemin started from −30 mV (Figure 2A), whereas the ill-defined wave of O_2 reduction at solely PEG-modified gold could be observed only from −150 mV (Figure S4).

In deaerated solutions, the aptamer-conjugated hemin showed two couple of peaks (Figure 2A, inset). A pronounced couple with a formal potential of −78 ± 6 mV (k_s of 0.07 s^{-1} based on 125 ± 6 mV peak separation[48] at 10 mV s^{-1}) was characteristic of the DNA-interacting hemin. Though no G4-hemin DNAzyme complex could be formed in the absence of thrombin, metalloporphyrins are also known to groove-bind and intercalate into the double stranded DNA (dsDNA).[49−51] The thrombin-specific aptamer can form a number of conformers possessing double-strand stem-loop structures (Figure S5) able of such hemin-dsDNA interactions shifting the redox potential of free hemin to more positive values. A less pronounced couple at ca. −350 mV approaches the potentials of hemin attached to SAMs of alkanethiols (and varying between −336 mV and −350 mV for different length SAMs)[34] that we ascribe to "free" hemin, i.e., DNA-conjugated but not interacting with DNA bases. Ca. 0.233 ± 0.061 pmol cm^{-2} of the hemin-conjugated aptamer was immobilized on the electrode surface, as determined from the hemin voltammetric signals at −78 mV in deaerated solutions, which increased almost 2-fold (to ca. 0.5 pmol cm^{-2}) when summarized voltammetric signals (−78 and −350 mV peaks) were taken into account (Figure 2A, inset).

As shown below, the aptamer/PEG-SH mixed SAM ensured the best antifouling properties against nonspecific protein

https://doi.org/10.1021/acsami.1c03784
ACS Appl. Mater. Interfaces XXXX, XXX, XXX−XXX

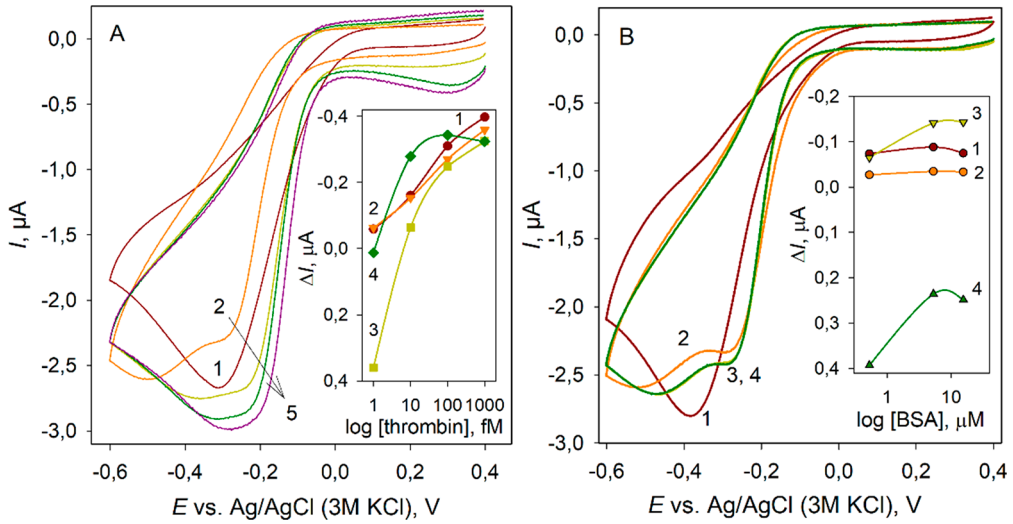

Figure 3. Representative CVs of the aptamer-hemin/PEG-modified gold electrodes in 20 mM PBS/0.15 M NaCl, pH 7.4, recorded in aerated solutions (0.27 mM O_2), (1) before and (2−5) after additions of (A): (2) 1, (3) 10, (4) 100 fM, and (5) 1 pM thrombin; (B): (2) 0.55, (3) 5.30, and (4) 15.15 μM BSA. Scan rate of 10 mV s^{-1}. Insets: Background-corrected current responses to (A) thrombin and (B) BSA additions at (1) 0.3, (2) 0.2, (3) −0.3, and (4) −0.4 V. In (4) the O_2-diffusion-limited saturation of the signal response with the thrombin concentration is seen.

adsorption, and this system was further used in the biosensor development.

Detection of Thrombin via Electrocatalytic Reduction of O_2 by the G4-Hemin Covalent Complexes Formed after Thrombin Binding. The direct O_2 bioelectrocatalytic activity (the "oxidase" activity) of the G4-hemin covalent complexes formed after thrombin binding was assessed in the air-equilibrated solutions containing ca. 0.27 mM O_2 expected from its 8.74 mg L^{-1} water solubility at 21 °C (Figure 3A). In contrast to the mixed aptamer/mercaptohexanol- and aptamer/diEG-modified electrodes, thrombin binding did not inhibit but enhanced the efficiency of electrocatalysis of O_2 reduction at the aptamer/PEG-modified electrodes, designating the formation of the G4-hemin DNAzyme complex and demonstrating its direct ET electrocatalytic activity not disturbed by protein nonspecific adsorption.

Two analytically significant potential regions could be seen in cyclic voltammograms (CVs): (1) from 0.4 to 0 V, and (2) from 0 to −0.6 V. In the first region, the currents consistently increased after thrombin binding, designating the formation of the DNAzyme complex that exhibited direct electrocatalytic activity in the reaction of O_2 reduction higher than that of "free", G4-unbound hemin. Within this potential region, the CV responses of the aptamer electrodes to thrombin linearly increased with the increasing logarithmic concentration of thrombin starting from its 1 fM levels (Figure 3A, inset, curves 1, 2). In the second region, the electrocatalysis enhancement was also observed. Therewith, the half-wave potential of electrocatalysis became less negative (a 41 ± 3 mV shift for 1 pM thrombin), whereas the electrocatalysis onset potentials remained the same. However, at the lowest femtomolar thrombin concentration, the CV variation within the second region was the opposite, which we ascribe to the dynamic nature of the CV analysis.

Dynamic polarization of biointerfaces may affect both the surface state/conformation of the aptamer complex and electrocatalysis in a less predictable way[37] than polarization at a constant potential applied[52] (Figure 3A versus Figure 3C). Apparently, within the second region (at the negative electrode potentials), the O_2 electrocatalysis based on direct ET between the electrode and the G4-hemin complex formed with a minute amount of thrombin, appeared to be very sensitive to polarization-induced interfacial changes. Those may be due to the polarization-induced either blocking of the electrode by the aptamer-thrombin complex or/and the conformational changes of the aptamer complex.[37] This effect disappeared at higher concentrations of thrombin when a larger number of the G4-hemin complexes were formed.

To avoid the dynamic-polarization-induced artifacts, we used the constant-potential polarization technique, chronocoulometry (CC). At potentials corresponding to the diffusion-limited electrocatalytic currents of O_2 reduction (≤−0.3 V, below the electrocatalytic peak potentials), the CC indicated that the electrocatalytic response of the aptamer electrodes to thrombin consistently increased with the increasing concentration of thrombin over whole thrombin concentration range studied (from 1 fM to 1 pM) (Figure 4A). The CC response Q of the system can be approximated as[53]

$$Q = (2nFAD_0^{1/2}C_0^{*}t^{1/2})/\pi^{1/2} + Q_{edl} + Q_{G4-hemin} \quad (1)$$

where the first summand stands for the electrocatalytic response (with D_0 being the diffusion coefficient of O_2 and C_0^* being its bulk concentration), whereas the second and third summands, Q_{edl} and $Q_{G4\text{-}hemin}$, stand for the charging of the electric double layer and redox transformation of the G4-hemin complex on the electrode surface. With time t, both Q_{edl} and $Q_{G4\text{-}hemin}$ become negligible compared to the first summand because of the more rapid electrocatalytic charge accumulation with t. Thus, CC inherently amplifies the read-out of the electrocatalytic signal and warrants an immediate and correct read-out of the aptamer electrode responses to thrombin additions (Figure 4A, C).

Bovine serum albumin, BSA, did not produce any protein-concentration related current amplification in CVs within potential regions (1) and (2), though, when the BSA concentration reached its sub-micromolar levels, a concentration-independent current enlargement could be observed starting from 0.4 to 0 V (in the magnitude similar to the addition of 1 fM thrombin). The latter was rather connected

https://doi.org/10.1021/acsami.1c03784
ACS Appl. Mater. Interfaces XXXX, XXX, XXX−XXX

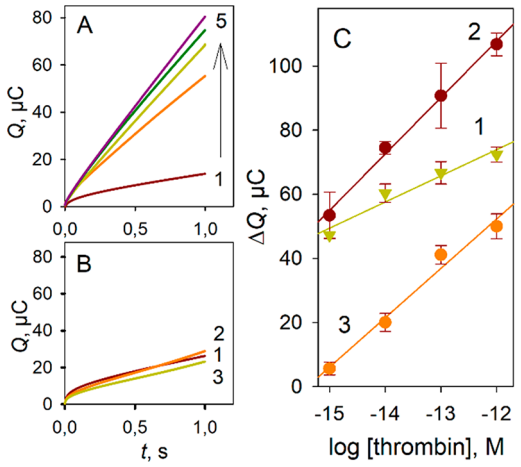

Figure 4. Representative CCs of the aptamer-hemin/PEG-modified gold electrodes in 20 mM PBS/0.15 M NaCl, pH 7.4, recorded in aerated solutions (0.27 mM O_2). (A, B) Representative CCs recorded (1) before and (2−5) after additions of (A) (2) 1, (3) 10, and (4) 100 fM and (5) 1 pM thrombin; (B) (1) 0, (2) 5.30, and (3) 15.15 μM BSA. E_{appl} = −0.4 V. (C) Background-corrected dependences of the CC signal change ΔQ on the logarithmic concentration of thrombin in (1) PBS, (2) 1% serum, and (3) CSF containing 6 μM dopamine, 35 μM uric acid, and 0.2 mM ascorbic acid.

with a biointerface restructuring resulting from nonspecific BSA interactions with the aptamer. The albumin amount in human serum ranges between 0.53 and 0.75 mM and in 100-fold diluted serum (further used in studies) should reach 5−7 μM levels.[37] However, no eventual increase of the electrocatalytic currents at negative electrode potentials could be seen in CVs (Figure 3B) and in CCs (Figure 4B) at those levels of BSA. Thus, those BSA concentrations did not boost electrocatalysis, consistent with no formation of the G4-hemin complexes.

Therefore, the reaction of electrocatalytic reduction of O_2 by the covalent G4-hemin complexes resulting from thrombin binding to its aptamer can be used for specific detection of thrombin indeed. This reaction is not completely identical to the peroxidase cycle[43,54,55] expected for the peroxidase DNAzyme activity.[23] However, it can still proceed through the formation of a higher oxidation state formed in the presence of the intermediate product of O_2 reduction − H_2O_2 - and stabilized by the G4-hemin complex similarly to the peroxidase catalysis and bioelectrocatalysis:[43,56]

$$\text{G4} - (\text{Fe(III)Porph}^{2-})^{+} + \text{H}_2\text{O}_2 \rightarrow \text{G4} - (\text{Fe(IV)} = \text{O}, \text{Porph}^{\bullet -})^{\bullet +} + \text{H}_2\text{O} \quad \text{(c)}$$

Here, the analogue of peroxidase compound 1, consisting of an oxyferryl iron (Fe^{4+}=O) and a porphyrin π cation radical, is presumably formed and then further reduced at the electrode surface in a $2e^-/2H^+$ reaction to ferric hemin starting from 0.4 V:

$$\text{G4} - (\text{Fe(IV)} = \text{O}, \text{Porph}^{\bullet -})^{\bullet +} + 2\text{e}^- + 2\text{H}^+ \rightarrow \text{G4} - (\text{Fe(III)Porph}^{2-})^{+} + \text{H}_2\text{O} \quad \text{(d)}$$

This reaction explains the consistently higher potential for the reaction of O_2 reduction (from 0.4 V, Figure 3A) compared to the G4-unbound hemin (from 0 V, Figure S3). Similarly higher onset potentials for the bioelectrocatalytic O_2 reduction, with two regions of a higher and lower electrocatalytic activity, were observed with some hemoglobins exhibiting both a pseudoperoxidase and oxidase electrocatalytic activity.[30,31]

Electroanalysis of Thrombin in Serum and CSF. To demonstrate the feasibility of the approach for practical analysis of thrombin, we tested the aptasensor performance in 1% human serum and in artificial CSF (Figure 5). Human serum diluted 100 times slightly affected the background signal observed with the aptamer electrodes in PBS, however, a pronounced enhancement of O_2 electrocatalysis could be followed after the aptamer electrode incubation in thrombin-containing serum solutions (Figure 5A). Eventually, electroanalysis of thrombin in serum showed the improved sensitivity compared to serum-free solutions (Figure 4C). The reason may be that serum proteins can intensify the process of forming the thrombin-aptamer complex and improve its

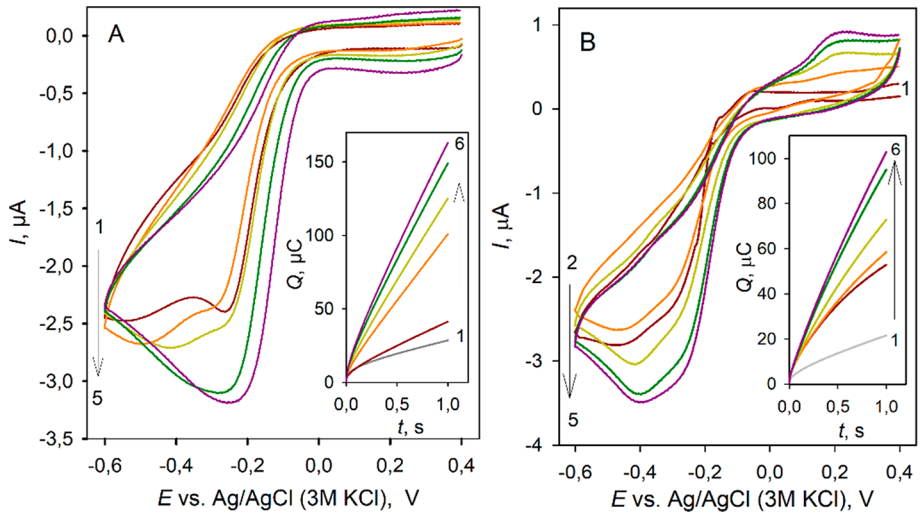

Figure 5. Representative CVs and (inset) CC of the hemin-aptamer/PEG-modified gold electrode recorded in (A) 20 mM PBS/0.15 M NaCl, pH 7.4, containing 1% human serum and in (B) artificial CSF, pH 7.4, containing 6 μM dopamine, 35 μM uric acid, and 0.2 mM ascorbic acid; (1, brown line) before and (2−5, insets 3−6) after additions of 1, 10, and 100 fM and 1 pM of thrombin. Insets: (1, gray line) responses in PBS and CSF and (2, brown line) after serum or interferents addition.

https://doi.org/10.1021/acsami.1c03784
ACS Appl. Mater. Interfaces XXXX, XXX, XXX−XXX

Table 1. Selected Examples of Ultrasensitive Electrochemical Aptasensors for Thrombin

electroanalytical scheme	technique	LOD[a], linear range	interferents/media	time	ref.
DNA-AuNP-modified GCE with target-triggering nicking enzyme signaling amplification with a Co-MOF/PtPd NPs label	DPV with H_2O_2 in solution	1 pM; 1 pM to 30 nM	10% serum	>9 h	18
sandwich aptamer assay with Pt NT/rGO-peptide/G4-hemin label	DPV with NADH, O_2, and hemin in solution	50 fM; 50 fM to 60 nM	10% serum; CEA; AFP, Hb	~1 h	19
proximity-binding displacement assay resulting in the formation of G4-hemin DNAzyme on Au	DPV with hemin in solution; N_2	10 pM; 0.01−50 nM	10% serum; human IgG, lysozyme, BSA	~3 h	25
sandwich aptamer assay with a AuNP/ZnONPs-G4-hemin/alkaline phosphatase label	DPV with hemin, H_2O_2, NP in solution	1 pM; 1 pM to 30 nM	10% serum; CEA; CA 19−9, BSA	~2 h	26
sandwich aptamer assay with a G4-hemin/MWCNT-MnO_2-PtNP label, H_2O_2 reduction	DPV, with hemin, H_2O_2 in solution	1 pM; 1 pM to 30 nM	10% serum; BSA, Hb, human IgG	1.5 h	16
sandwich DNA-aptamer displacement assay on CdS films, with AuNP labels	ECL with persulfate in solution	0.1 fM; 0.1−100 fM	PBS, pH 8; 1 pM BSA, Hb, and lysozyme	40 min	65
aptamer-modified PbS QDs assembled on an ITO electrode; basis: ET from photoexcited PbS to G4-hemin reducing O_2	photocurrent, hemin and O_2 in solution	1 pM; 1 pM to 10 nM	Tris, pH 7.4; 0.1 nM IgG or BSA, 0.1 mM L-Cys	50 min	66
O_2 electrocatalysis by the DNAzyme complex formed at hemin-conjugated aptamer/PEG-modified electrode	CC at −0.4 V, with O_2	1 fM; 1 fM to 1 pM	1% serum; BSA; CSF; dopamine, uric and ascorbic acid	30 min	here

[a]The LOD is cited in accordance with the IUPAC definition as "the smallest amount of concentration of analyte in the sample that can be reliably distinguished from zero". Abbreviations: AFP, alpha-fetoprotein antigen; CA, carbohydrate antigen; CC, chronocoulometry; CEA, carcinoembryonic antigen; CSF, cerebrospinal fluid; DPV, differential pulse voltammetry; ECL, electrochemiluminescence; GCE, glassy carbon electrode; Hb, hemoglobin; ITO, indium tin oxide; MOF, metal−organic framework; MWCNT, multiwall carbon nanotubes; NP, 1-naphthyl phosphate; NPs, nanoparticles; QDs, quantum dots; rGO, reduced graphene oxide.

stability.[57,58] The experimentally observed LOD of 1 fM thrombin allows direct analysis of serum samples prepared by 100-fold dilution, as the thrombin content in human serum ranges between below sub-picomolar levels in healthy individuals[59,60] and sub-nanomolar to hundreds of nanomolars during surgery activating the clotting system and coagulation.[11,60] The recovery efficacy determined by standard additions of 5 fM and 50 fM thrombin (using its 50 pM stock solution in serum) to 1 fM thrombin samples, in 1% human serum, was 96 ± 2% and 105 ± 3%, which was sufficiently accurate for perspective bioanalytical applications. (NB: the typical immunoassay recovery acceptance range is 80−120%).

In CSF, small-molecule interferents such as catecholamines (up to 2−6 μM), ascorbic acid (ca. 0.2−0.3 mM), and uric acid (up to 20−42 μM)[40,61,62] could strongly affect the electrocatalytic activity of G4-hemin complexes, and the aptasensor performance in CSF was tested in their presence. Although artificial CSF itself and uric acid did not essentially change the electrocatalytic background signals, both dopamine and ascorbic acid contributed to the background CVs with distinct oxidation signals at 0.1 V (the characteristic potential for dopamine oxidation)[63] and −0.1 V (ascorbic acid oxidation)[64] (Figure S6). In addition, the O_2 reduction wave (the current signal at −0.4 V) was enhanced in the dopamine-containing solutions, suggesting the mediating role of this catecholamine in electrocatalysis (Figure S6C). On the other hand, the addition of the excessive (to dopamine) concentration of ascorbic acid, known to be a free-radical scavenger, interfered with this role and diminished the O_2-reduction signal to the CSF background levels (Figure S6D).

In artificial CSF containing all interferents, the formation of the G4-hemin complex in thrombin-containing solutions resulted in the enhanced electrocatalysis of O_2 reduction by the formed DNAzyme complexes, and this enhancement was proportional to the added amounts of thrombin (Figure 5B). Therewith, the consistently increasing electrocatalytic oxidation of dopamine could be also followed starting from 0 V suggesting that the formed DNAzyme can also electrocatalyze oxidation of catechols in the presence of O_2 (Figure 5B). At fixed, physiologically relevant concentrations of dopamine, uric acid, and ascorbic acid, their presence did not interfere with thrombin analysis at −0.4 V (Figure 5B, inset). Analysis showed 94 ± 3% and 110 ± 5% recovery of interferent-containing CSF samples spiked with 5 and 50 fM thrombin. It is worth noting that although all studied by us media allowed practical determination of down to 1 fM thrombin, the best sensitivity of analysis was in serum (17.83 μC/log[thrombin], M) and CSF (15.42 μC/log[thrombin], M), with the lowest sensitivity shown in phosphate buffer solutions (8.18 μC/log[thrombin], M) (Figure 4C).

Thus, the shown oxidase activity of the covalent G4-hemin complexes naturally formed by the aptamer and thrombin allows simple and robust CC detection of femtomolar levels of thrombin both in diluted serum and in artificial CSF containing dopamine, uric acid, and ascorbic acid. The assay is virtually label-free, i.e., it does not require any extra reagents/redox indicators or mediators present in solution and does not need any working solution deaeration, essential in the assays based on peroxidase activity of the G4-hemin DNAzymes. Its sole dependence on atmospheric O_2 simplifies and shortens the analytical procedure, once the experimental conditions, such as constant temperature and sufficient air-equilibration times, support the constant concentration of the dissolved O_2 in working solutions, and it can be easily adapted both for microelectrode and microelectronic chip/microfluidic formats. On the other hand, its O_2 dependence makes it less suitable for direct in vivo applications, in which sufficient fluctuations of oxygen levels may be expected.

In terms of the sensitivity/LOD, time of analysis, simplicity, and eventually, its cost, the assay successfully competes with currently existing electrochemical approaches for thrombin detection exploiting a variety of electrocatalytic and enzymatic amplification schemes (Table 1), which makes it highly suitable for immediate clinical applications.

https://doi.org/10.1021/acsami.1c03784
ACS Appl. Mater. Interfaces XXXX, XXX, XXX−XXX

However, it is clear that any potential clinical applications require a further assay development, such as its adaptation to commercial electrodes or disposable screen-printed or microelectronically produced ones. Considering a very different quality of these electrode surfaces, it will require adjustments of immobilization protocols. Another related issue is a limited operational and long-term stability of bioelectrodes based on gold-immobilized thiolated aptamers. A 23−30% signal loss due to DNA desorption is routinely observed after 4−5 days of storage of the thiolated DNA/mercaptohexanol electrodes.[67,68] Multiple sulfur−gold binding tags, such as phosphoro-thioated dA_x or trithiols, improve the SAM stability just a little, with then from 15[67] to 20%[68] DNA loss after 4−5 days of storage. The thiolated aptamer/thiolated PEG electrode modification used here showed better stability, with no significant signal loss within 5 days of storage (see Materials and Methods and Figure S7). However, it may be still insufficient for a long-term (several months) storage of the modified electrodes, and additional stabilization agents should be sought.

More cost-effective analysis such as continuous monitoring of thrombin in flow-injection and flow-through systems also requests the possibility of electrodes' regeneration. We tested several regeneration protocols, including washing in water, 7 M urea, and 6 M guanidinium chloride. The latter allowed a full restoration of the aptamer electrode background signal, consistent with previous reports.[12] Therewith, the operational stability of the regenerated bioelectrodes was compromised by the necessity of their constant removal from the working media for regeneration accompanied by their concomitant exposure to the air promoting corrosive desorption of the aptamer, with a signal dropping down 34% after 4 cycles of detection/regeneration (Figure S7). Nevertheless, the promising results on the regeneration possibility combined with an improved operational stability achievable in a flow (such as shown by continuous 20 h monitoring of dopamine by the aptamer electrodes with just a 10% signal loss)[69] outlines further directions for the practical clinical assay development.

CONCLUSIONS

Here, we demonstrated that the "oxidase" activity of the covalent G4-hemin DNAzyme complex, naturally formed by the thrombin aptamer and its ligand, provides more efficient electrocatalysis of O_2 reduction than free hemin's one and at potentials 0.5 V higher. The ability of this DNAzyme to directly, with no mediators, electrocatalyze O_2 reduction was for the first time applied for the protein detection in serum and CSF. At the hemin-conjugated aptamer- and PEG-modified gold electrodes, down to 1 fM thrombin could be detected by chronocoulometry at −0.4 V in aerated buffer solutions, 1% serum, and artificial CSF containing physiological levels of dopamine, uric acid, and ascorbic acid. This basic approach of using the reaction of electrocatalytic reduction of O_2 catalyzed by G4-hemin covalent complexes offers a new tool for ultrasensitive electrocatalytic assays in which simple and efficient O_2-dependent DNAzyme labels can be used.

ASSOCIATED CONTENT

Supporting Information

The Supporting Information is available free of charge at https://pubs.acs.org/doi/10.1021/acsami.1c03784.

ESI-TOFF spectrum for the aptamer; characterization of bioconjugates; CV of bare and PEG-modified gold electrodes in aerated and deaerated solutions; aptamer conformations predicted by DINAMelt calculations; CV responses of the hemin-aptamer/PEG-modified electrodes in artificial CSF; repeatability data (PDF)

AUTHOR INFORMATION

Corresponding Author

Elena E. Ferapontova − *Interdisciplinary Nanoscience Center (iNANO), Science and Technology, Aarhus University, Aarhus C DK-8000, Denmark;* orcid.org/0000-0003-1177-3204; Phone: (+45) 87156703; Email: elena.ferapontova@inano.au.dk

Author

Kamila Malecka − *Interdisciplinary Nanoscience Center (iNANO), Science and Technology, Aarhus University, Aarhus C DK-8000, Denmark; Institute of Animal Reproduction and Food Research, Polish Academy of Sciences, Olsztyn 10-748, Poland*

Complete contact information is available at: https://pubs.acs.org/10.1021/acsami.1c03784

Notes

The authors declare no competing financial interest.

ACKNOWLEDGMENTS

This work was supported by the Danish Council for Independent Research (DFF-FTP-4005-00482B). K.M. acknowledges the support from the KNOW consortium 'Healthy Animal—Safe Food' MS&HE no. 05-1/KNOW2/2015.

REFERENCES

(1) Prince, M.; Bryce, R.; Albanese, E.; Wimo, A.; Ribeiro, W.; Ferri, C. P. The Global Prevalence of Dementia: A Systematic Review and Metaanalysis. *Alzheimer's Dementia* **2013**, *9*, 63−75.e2.

(2) Humpel, C. Chronic Mild Cerebrovascular Dysfunction as a Cause for Alzheimer's Disease? *Exp. Gerontol.* **2011**, *46*, 225−232.

(3) Pimentel-Coelho, P. M.; Rivest, S. The Early Contribution of Cerebrovascular Factors to the Pathogenesis of Alzheimer's Disease. *Eur. J. Neurosci.* **2012**, *35*, 1917−1937.

(4) Grammas, P. Neurovascular Dysfunction, Inflammation and Endothelial Activation: Implications for the Pathogenesis of Alzheimer's Disease. *J. Neuroinflammation* **2011**, *8*, No. 26.

(5) Di Cera, E. Thrombin. *Mol. Aspects Med.* **2008**, *29*, 203−254.

(6) Grammas, P.; Martinez, J. M. Targeting Thrombin: an Inflammatory Neurotoxin in Alzheimer's Disease. *J. Alzheimer's Dis.* **2014**, *42*, S537−S544.

(7) Deng, B.; Lin, Y.; Wang, C.; Li, F.; Wang, Z.; Zhang, H.; Li, X.-F.; Le, X. C. Aptamer Binding Assays for Proteins: The Thrombin Example—A Review. *Anal. Chim. Acta* **2014**, *837*, 1−15.

(8) Mann, K. G. Thrombin Generation in Hemorrhage Control and Vascular Occlusion. *Circulation* **2011**, *124*, 225−235.

(9) Leiba, M.; Malkiel, S.; Budnik, I.; Rozic, G.; Avigdor, A.; Duek, A.; Nagler, A.; Kenet, G.; Livnat, T. Thrombin Generation as a Predictor of Thromboembolic Events in Multiple Myeloma Patients. *Blood Cells, Mol., Dis.* **2017**, *65*, 1−7.

(10) Nierodzik, M. L.; Karpatkin, S. Thrombin Induces Tumor Growth, Metastasis, and Angiogenesis: Evidence for a Thrombin-Regulated Dormant Tumor Phenotype. *Cancer Cell* **2006**, *10*, 355−362.

(11) Wolberg, A. S.; Campbell, R. A. Thrombin Generation, Fibrin Clot Formation and Hemostasis. *Transfus. Apher. Sci.* **2008**, *38*, 15−23.

(12) Xiao, Y.; Lubin, A. A.; Heeger, A. J.; Plaxco, K. W. Label-Free Electronic Detection of Thrombin in Blood Serum by Using an Aptamer-Based Sensor. *Angew. Chem., Int. Ed.* **2005**, *44*, 5456−5459.
(13) Radi, A.-E.; Acero Sánchez, J. L.; Baldrich, E.; O'Sullivan, C. K. Reagentless, Reusable, Ultrasensitive Electrochemical Molecular Beacon Aptasensor. *J. Am. Chem. Soc.* **2006**, *128*, 117−124.
(14) Striggow, F.; Riek, M.; Breder, J.; Henrich-Noack, P.; Reymann, K. G.; Reiser, G. The Protease Thrombin is an Endogenous Mediator of Hippocampal Neuroprotection against Ischemia at Low Concentrations but Causes Degeneration at High Concentrations. *Proc. Natl. Acad. Sci. U. S. A.* **2000**, *97*, 2264−2269.
(15) Krenzlin, H.; Lorenz, V.; Danckwardt, S.; Kempski, O.; Alessandri, B. The Importance of Thrombin in Cerebral Injury and Disease. *Int. J. Mol. Sci.* **2016**, *17*, No. 84.
(16) Xu, W.; Xue, S.; Yi, H.; Jing, P.; Chai, Y.; Yuan, R. A Sensitive Electrochemical Aptasensor Based on the Co-Catalysis of Hemin/G-Quadruplex, Platinum Nanoparticles and Flower-Like MnO_2 Nanosphere Functionalized Multi-Walled Carbon Nanotubes. *Chem. Commun.* **2015**, *51*, 1472−1474.
(17) Heydari-Bafrooei, E.; Amini, M.; Ardakani, M. H. An Electrochemical Aptasensor Based on TiO_2/MWCNT and a Novel Synthesized Schiff Base Nanocomposite for the Ultrasensitive Detection of Thrombin. *Biosens. Bioelectron.* **2016**, *85*, 828−836.
(18) Yang, X.; Lv, J.; Yang, Z.; Yuan, R.; Chai, Y. A Sensitive Electrochemical Aptasensor for Thrombin Detection Based on Electroactive Co-Based Metal−Organic Frameworks with Target-Triggering NESA Strategy. *Anal. Chem.* **2017**, *89*, 11636−11640.
(19) Wu, Y.; Zou, L.; Lei, S.; Yu, Q.; Ye, B. Highly Sensitive Electrochemical Thrombin Aptasensor Based on Peptide-Enhanced Electrocatalysis of Hemin/G-Quadruplex and Nanocomposite as Nanocarrier. *Biosens. Bioelectron.* **2017**, *97*, 317−324.
(20) Nsabimana, A.; Ma, X.; Yuan, F.; Du, F.; Abdussalam, A.; Lou, B.; Xu, G. Nanomaterials-Based Electrochemical Sensing of Cardiac Biomarkers for Acute Myocardial Infarction: Recent Progress. *Electroanalysis* **2019**, *31*, 177−187.
(21) Russo Krauss, I.; Pica, A.; Merlino, A.; Mazzarella, L.; Sica, F. Duplex-Quadruplex Motifs in a Peculiar Structural Organization Cooperatively Contribute to Thrombin Binding of a DNA Aptamer. *Acta Crystallogr., Sect. D: Biol. Crystallogr.* **2013**, *69*, 2403−2411.
(22) Bode, W.; Mayr, I.; Baumann, U.; Huber, R.; Stone, S. R.; Hofsteenge, J. The Refined 1.9 A Crystal Structure of Human Alpha-Thrombin: Interaction with D-Phe-Pro-Arg Chloromethylketone and Significance of the Tyr-Pro-Pro-Trp Insertion Segment. *EMBO J.* **1989**, *8*, 3467−3475.
(23) Travascio, P.; Li, Y.; Sen, D. DNA-Enhanced Peroxidase Activity of a DNA Aptamer-Hemin Complex. *Chem. Biol.* **1998**, *5*, 505−517.
(24) Golub, E.; Freeman, R.; Niazov, A.; Willner, I. Hemin/G-Quadruplexes as DNAzymes for the Fluorescent Detection of DNA, Aptamer−Thrombin Complexes, and Probing the Activity of Glucose Oxidase. *Analyst* **2011**, *136*, 4397−4401.
(25) Yang, J.; Dou, B.; Yuan, R.; Xiang, Y. Proximity Binding and Metal Ion-Dependent DNAzyme Cyclic Amplification-Integrated Aptasensor for Label-Free and Sensitive Electrochemical Detection of Thrombin. *Anal. Chem.* **2016**, *88*, 8218−8223.
(26) Yang, Z.-H.; Zhuo, Y.; Yuan, R.; Chai, Y.-Q. Amplified Thrombin Aptasensor Based on Alkaline Phosphatase and Hemin/G-Quadruplex-Catalyzed Oxidation of 1-Naphthol. *ACS Appl. Mater. Interfaces* **2015**, *7*, 10308−10315.
(27) Pelossof, G.; Tel-Vered, R.; Elbaz, J.; Willner, I. Amplified Biosensing Using the Horseradish Peroxidase-Mimicking DNAzyme as an Electrocatalyst. *Anal. Chem.* **2010**, *82*, 4396−4402.
(28) Gribas, A. V.; Zhao, S.; Sakharov, I. Y. Improved Method for Chemiluminescent Determination of Peroxidase-Mimicking DNAzyme Activity. *Anal. Biochem.* **2014**, *466*, 19−23.
(29) Fapyane, D.; Kékedy-Nagy, L.; Sakharov, I. Y.; Ferapontova, E. E. Electrochemistry and Electrocatalysis of Covalent Hemin-G4 Complexes on Gold. *J. Electroanal. Chem.* **2018**, *812*, 174−179.
(30) Fernandez, E.; Larsson, J. T.; McLean, K. J.; Munro, A. W.; Gorton, L.; von Wachenfeldt, C.; Ferapontova, E. E. Electron Transfer Reactions, Cyanide and O_2 Binding of Truncated Hemoglobin from *Bacillus subtilis*. *Electrochim. Acta* **2013**, *110*, 86−93.
(31) Sosna, M.; Leiva-Eriksson, N.; Bülow, L.; Ferapontova, E. E. Electrochemical Characterization and Bioelectrocatalytic H_2O_2 Sensing of Non-Symbiotic Hexa-Coordinated Sugar Beet Hemoglobins. *ChemElectroChem* **2020**, *7*, 2114−2122.
(32) Tasset, D. M.; Kubik, M. F.; Steiner, W. Oligonucleotide Inhibitors of Human Thrombin that Bind Distinct Epitopes. *J. Mol. Biol.* **1997**, *272*, 688−698.
(33) Fenton, J. W., 2nd; Fasco, M. J.; Stackrow, A. B. Human Thrombins. Production, Evaluation, and Properties of Alpha-Thrombin. *J. Biol. Chem.* **1977**, *252*, 3587−3598.
(34) Sosna, M.; Fapyane, D.; Ferapontova, E. E. Reconstitution of Peroxidase onto Hemin-Terminated Alkanethiol Self-Assembled Monolayers on Gold. *J. Electroanal. Chem.* **2014**, *728*, 18−25.
(35) Fapyane, D.; Ferapontova, E. E. Enhanced Electron Transfer Between Gold Nanoparticles and Horseradish Peroxidase Reconstituted onto Alkanethiol-Modified Hemin. *Electrochem. Commun.* **2016**, *70*, 39−42.
(36) Jarczewska, M.; Kekedy-Nagy, L.; Nielsen, J. S.; Campos, R.; Kjems, J.; Malinowska, E.; Ferapontova, E. E. Electroanalysis of pM-Levels of Urokinase Plasminogen Activator in Serum by Phosphorothioated RNA aptamer. *Analyst* **2015**, *140*, 3794−3802.
(37) Salimian, R.; Kékedy-Nagy, L.; Ferapontova, E. E. Specific Picomolar Detection of a Breast Cancer Biomarker HER-2/neu Protein in Serum: Electrocatalytically Amplified Electroanalysis by the Aptamer/PEG-Modified Electrode. *ChemElectroChem* **2017**, *4*, 872−879.
(38) Wakui, K.; Yoshitomi, T.; Yamaguchi, A.; Tsuchida, M.; Saito, S.; Shibukawa, M.; Furusho, H.; Yoshimoto, K. Rapidly Neutralizable and Highly Anticoagulant Thrombin-Binding DNA Aptamer Discovered by MACE SELEX. *Mol. Ther.–Nucleic Acids* **2019**, *16*, 348−359.
(39) Álvarez-Martos, I.; Møller, A.; Ferapontova, E. E. Dopamine Binding and Analysis in Undiluted Human Serum and Blood by the RNA-Aptamer Electrode. *ACS Chem. Neurosci.* **2019**, *10*, 1706−1715.
(40) Álvarez-Martos, I.; Ferapontova, E. E. Negative Electrocatalysis"-Based Specific Analysis of Dopamine at Basal Plane HOPG in the Presence of Structurally Related Catecholamines. *Electrochem. Commun.* **2018**, *89*, 48−51.
(41) Gribas, A. V.; Korolev, S. P.; Zatsepin, T. S.; Gottikh, M. B.; Sakharov, I. Y. Structure−Activity Relationship Study for Design of Highly Active Covalent Peroxidase-Mimicking DNAzyme. *RSC Adv.* **2015**, *5*, 51672−51677.
(42) Luo, X.; Xu, Q.; James, T.; Davis, J. J. Redox and Label-Free Array Detection of Protein Markers in Human Serum. *Anal. Chem.* **2014**, *86*, 5553−5558.
(43) Ferapontova, E. E. Direct Peroxidase Bioelectrocatalysis on a Variety of Electrode Materials. *Electroanalysis* **2004**, *16*, 1101−1112.
(44) Shipovskov, S.; Ferapontova, E. E. Biocatalysis of Theophylline Oxidation by Microbial Theophylline Oxidase in the Presence of Non-Physiological Electron Acceptors. *Biocatal. Biotransform.* **2008**, *26*, 455−465.
(45) Fapyane, D.; Kartashov, A.; von Wachenfeldt, C.; Ferapontova, E. E. Gated Electron Transfer Reactions of Truncated Hemoglobin from *Bacillus subtilis* Differently Orientated on SAM-Modified Electrodes. *Phys. Chem. Chem. Phys.* **2015**, *17*, 15365−15374.
(46) Forbes, L. M.; Sattayasamitsathit, S.; Xu, P. F.; O'Mahony, A.; Samek, I. A.; Kaufmann, K.; Wang, J.; Cha, J. N. Improved Oxygen Reduction Reaction Activities with Amino Acid R Group Functionalized PEG at Platinum Surfaces. *J. Mater. Chem. A* **2013**, *1*, 10267−10273.
(47) Pering, S. R.; Nicholas, J. A.; Bayatsarmadi, B.; Evans, D.; Fabretto, M.; Blencowe, A.; Murphy, P. J.; Talemi, P. The Effect of Block Copolymer Additives for a Highly Active Polymeric Metal-Free Oxygen Reduction Electrode. *RSC Adv.* **2016**, *6*, 28809−28814.

https://doi.org/10.1021/acsami.1c03784
ACS Appl. Mater. Interfaces XXXX, XXX, XXX−XXX

(48) Laviron, E. General Expression of the Linear Potential Sweep Voltammogram in the Case of Diffusionless Electrochemical Systems. *J. Electroanal. Chem. Interfacial Electrochem.* **1979**, *101*, 19−28.
(49) Pasternack, R. F.; Gibbs, E. J.; Villafranca, J. J. Interactions of Porphyrins with Nucleic Acids. *Biochemistry* **1983**, *22*, 5409−5417.
(50) Pasternack, R. F.; Brigandi, R. A.; Abrams, M. J.; Williams, A. P.; Gibbs, E. J. Interactions of Porphyrins and Metalloporphyrins with Single-Stranded Poly(dA). *Inorg. Chem.* **1990**, *29*, 4483−4486.
(51) Hudson, B. P.; Sou, J.; Berger, D. J.; McMillin, D. R. Luminescence Studies of the Intercalation of Cu(TMpyP4) into DNA. *J. Am. Chem. Soc.* **1992**, *114*, 8997−9002.
(52) Kékedy-Nagy, L.; Sørensen, K. D.; Ferapontova, E. E. Picomolar Sensitive and SNP-Selective "Off-On" Hairpin Genosensor Based on Structure-Tunable Redox Indicator Signals. *Biosens. Bioelectron.* **2018**, *117*, 444−449.
(53) Anson, F. C. Innovations in the Study of Adsorbed Reactants by Chronocoulometry. *Anal. Chem.* **1966**, *38*, 54−57.
(54) Ferapontova, E. E.; Castillo, J.; Hushpulian, D.; Tishkov, V.; Chubar, T.; Gazaryan, I.; Gorton, L. Direct Electrochemistry of Recombinant Tobacco Peroxidase on Gold. *Electrochem. Commun.* **2005**, *7*, 1291−1297.
(55) Ferapontova, E. E.; Grigorenko, V. G.; Egorov, A. M.; Börchers, T.; Ruzgas, T.; Gorton, L. Direct Electron Transfer in the System Gold Electrode−Recombinant Horseradish Peroxidases. *J. Electroanal. Chem.* **2001**, *509*, 19−26.
(56) Noble, R. W.; Gibson, Q. H. The Reaction of Ferrous Horseradish Peroxidase with Hydrogen Peroxide. *J. Biol. Chem.* **1970**, *245*, 2409−13.
(57) Wang, H.; Lu, M.; Weinfeld, M.; Le, X. C. Enhancement of Immunocomplex Detection and Application to Assays for DNA Adduct of Benzo[a]pyrene. *Anal. Chem.* **2003**, *75*, 247−254.
(58) Song, M.; Zhang, Y.; Li, T.; Wang, Z.; Yin, J.; Wang, H. Highly Sensitive Detection of Human Thrombin in Serum by Affinity Capillary Electrophoresis/Laser-Induced Fluorescence Polarization using Aptamers as Probes. *J. Chromatogr. A* **2009**, *1216*, 873−878.
(59) Rühl, H.; Müller, J.; Harbrecht, U.; Fimmers, R.; Oldenburg, J.; Mayer, G.; Pötzsch, B. Thrombin Inhibition Profiles in Healthy Individuals and Thrombophilic Patients. *Thromb. Haemostasis* **2012**, *107*, 848−853.
(60) Königsbrügge, O.; Koder, S.; Riedl, J.; Panzer, S.; Pabinger, I.; Ay, C. A New Measure for *In Vivo* Thrombin Activity in Comparison with *In Vitro* Thrombin Generation Potential in Patients with Hyper- and Hypocoagulability. *Clin. Exp. Med.* **2017**, *17*, 251−256.
(61) Hashimoto, K.; Ishima, T.; Sato, Y.; Bruno, D.; Nierenberg, J.; Marmar, C. R.; Zetterberg, H.; Blennow, K.; Pomara, N. Increased Levels of Ascorbic Acid in the Cerebrospinal Fluid of Cognitively Intact Elderly Patients with Major Depression: a Preliminary Study. *Sci. Rep.* **2017**, *7*, No. 3485.
(62) Tsunoda, S.; Gega, A.; Utsumi, S.; Matsuoka, Y.; Kubota, C. Diagnostic Value of the CSF Uric Acid Level. *No Shinkei Geka* **1978**, *6*, 971−974.
(63) Alvarez-Martos, I.; Campos, R.; Ferapontova, E. E. Surface State of the Dopamine RNA Aptamer Affects Specific Recognition and Binding of Dopamine by the Aptamer-Modified Electrodes. *Analyst* **2015**, *140*, 4089−4096.
(64) Álvarez-Martos, I.; Ferapontova, E. E. Electrocatalytic Discrimination between Dopamine and Norepinephrine at Graphite and Basal Plane HOPG Electrodes. *Electroanalysis* **2018**, *30*, 1082−1090.
(65) Wang, J.; Shan, Y.; Zhao, W.-W.; Xu, J.-J.; Chen, H.-Y. Gold Nanoparticle Enhanced Electrochemiluminescence of CdS Thin Films for Ultrasensitive Thrombin Detection. *Anal. Chem.* **2011**, *83*, 4004−4011.
(66) Wang, G.-L.; Shu, J.-X.; Dong, Y.-M.; Wu, X.-M.; Zhao, W.-W.; Xu, J.-J.; Chen, H.-Y. Using G-Quadruplex/Hemin To "Switch-On" the Cathodic Photocurrent of p-Type PbS Quantum Dots: Toward a Versatile Platform for Photoelectrochemical Aptasensing. *Anal. Chem.* **2015**, *87*, 2892−2900.
(67) Campos, R.; Kotlyar, A.; Ferapontova, E. E. DNA-Mediated Electron Transfer in DNA Duplexes Tethered to Gold Electrodes via Phosphorothioated dA Tags. *Langmuir* **2014**, *30*, 11853−11857.
(68) Phares, N.; White, R. J.; Plaxco, K. W. Improving the Stability and Sensing of Electrochemical Biosensors by Employing Trithiol-Anchoring Groups in a Six-Carbon Self-Assembled Monolayer. *Anal. Chem.* **2009**, *81*, 1095−1100.
(69) Álvarez-Martos, I.; Ferapontova, E. E. Electrochemical Label-Free Aptasensor for Specific Analysis of Dopamine in Serum in the Presence of Structurally Related Neurotransmitters. *Anal. Chem.* **2016**, *88*, 3608−3616.

https://doi.org/10.1021/acsami.1c03784
ACS Appl. Mater. Interfaces XXXX, XXX, XXX−XXX